Pergamon

Solid State Communications, Vol. 99, No. 11, pp. 853–857, 1996

0038-1098/96 $12.00+.00

PII: S0038-1098(96)00143-3

SCANNING ELECTRON ACOUSTIC MICROSCOPY OF SEMICONDUCTOR MATERIALS

Shuwei Li*[a], Fuming Jiang[b], Qingrui Yin[b] and Yixin Jin[a]

[a]Chang Chun Institute of Physics, Academia Sinica, 130021 Chang Chun, P.R. China
[b]Shang Hai Institute of Ceramics, Academia Sinica, 200050 Shang Hai, P.R. China

(*Received* 1 *December* 1995 *by L. Keldysh*)

The capability of scanning electron acoustic microscopy in semiconductor materials has been studied. The signal generation mechanisms and applications of scanning electron acoustic microscopy in *n*-GaSb (Te-doped) crystals, and GaInAsSb on GaSb, GaSb on GaAs and InSb epilayer on a GaAs substrate are investigated, which shows the new technique for image and characterization of thermal, elastic and pyroelectric property variations on a microscale resolution. Copyright © 1996 Elsevier Science Ltd

Keywords: A. semiconductors, A. surfaces and interfaces, D. acoustic properties.

1. INTRODUCTION

Scanning electron acoustic microscopy (SEAM), also referred to as thermal wave microscopy, was developed in 1980 [1] and has been used in recent years for the characterization of many materials. Urchulutegui and Piqueras *et al.* have studied subgrain boundaries and deformed regions of Mg, ZnO and SiC materials [2–4], grain and twin boundaries of GaP and InP semiconductor materials [5] and magnetic domains of magnetostriction samples [6]. Cantrell *et al.* have reported SEAM observations of indentations in ceramic [7]. A few SEAM observations of ionic crystals have been reported although this technique can be used to detect features such as cracks, deformed regions, precipitates, bubbles, etc. [8]. In this communication we report more detailed signal generation mechanisms and applications of SEAM in *n*-GaSb crystals and other semiconductor materials.

2. SIGNAL GENERATION MECHANISMS OF SEAM

SEAM as a new experimental tool has been successively reported for the study of polarization distribution, phase transition, subgrain boundaries and domain structure in polar materials and nondestructive observation of internal phenomena in many other materials and devices. Figure 1 shows the experimental SEAM arrangement used in this work. It was modified from a KyKy-1000B microscope made by a China–USA joint-venture company for showing electron-acoustic signals simultaneously. SEAM was constructed by us using conventional scanning electron microscopy (SEM) to which several newly designed parts, a flexible plug-in beam blanking system, an opto-electric coupler and a spring loaded and metal shielded PZT electron-acoustic signal detector were attached. The chopping system consists of a pair of condensor plates and beam blanking electronics to create a periodic beam. A function generator was used to produce a square-wave voltage with frequencies from 30 to 500 KHz. The sample of *n*-GaSb crystal is exposed to a focused, intensity modulated beam from an electron gun. As the beam is scanned across the surface, energy is absorbed at or near the surface of the sample and local periodic heating and thermal expansion occur. The chopping of the electron beam generates both acoustic and thermal waves in the sample clamped on a piezoelectric ceramic transducer (PZT). Thermal waves are highly-damped waves, travel only within thermal wavelengths and interact with thermal features of the surroundings within their range. Thermal wave

* Corresponding author.

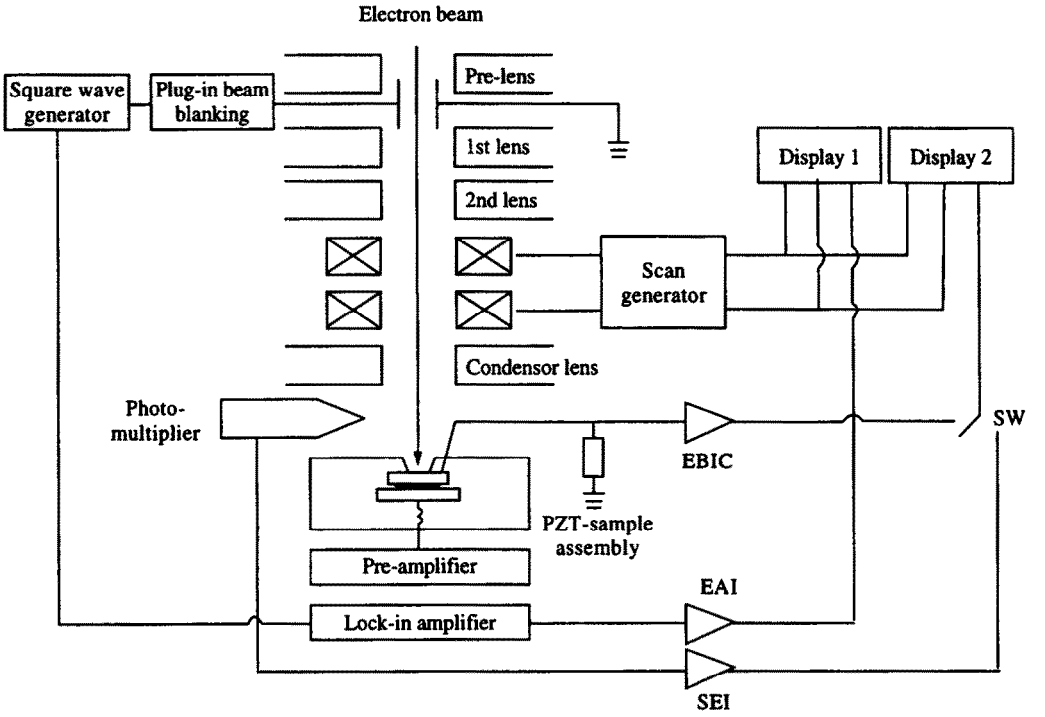

Fig. 1. SEAM experimental setup.

behaviors are controlled by the frequency at which the electron beam is modulated and their wavelengths decrease as the frequency increases. In addition to modulation frequency dependence, the thermal wave characteristics are controlled by the thermal properties, especially thermal conductivity, of the material examined. Thus, any feature on or beneath the sample surface, but with the thermal wave's propagation range with thermal characteristics different from its surroundings, will reflect and scatter the thermal waves. Because the periodic heating, which produces thermal waves, introduces periodic stress–strain conditions in the heated region, the acoustic signals are derived from thermal waves. The thermal wave component generated in the material is highly attenuated, so that in practice the information recorded from the transducer attached to a thermally thick sample depends on the received acoustic wave component. The acoustic waves travel far into the solid and may be readily detected. The amplification is carried out by a low-noise preamplifer installed inside the electron gun, a lock-in amplifier receiving the reference signal f from the function generator and a video amplifier for recording and displaying. The signal was detected at the reference f or at $2f$. The acoustic signal was measured with the upper side of the sample earthed and the specimen transducer interface unearthed. With the amplitude A and the phase delay ϕ of the detected signal with respect to the reference square wave alternative images can be formed.

3. SEAM RESULTS AND DISCUSSION OF *n*-GaSb

The electron-acoustic imaging was performed on a conventional scanning electron microscope attached by several newly designed parts. Since SEAM is an accessory to the SEM, it allows direct comparison of images obtained. Figure 2 show the SEM and SEAM image of the same area of the *n*-GaSb crystal. The electron beam characteristics were chopping frequency from 30 to 500 KHz, duty ratio of 50%, acceleration voltage of 20–30 KV, and maximum beam current of $4 \times 10\,\mu$A. Comparison of SEM and SEAM images shows that the two techniques provide different information. The *n*-GaSb crystal was substrate doped Te and oriented 2–3° (1 0 0) towards ⟨1 1 0⟩. The figure 2(B) SEAM image shows light and shade contrast at the upper left and the lower right, it is caused by the change of doped density. The SEAM signal generation mechanism has been explained by the conversion of an electron-beam-induced heat distribution into sound. In the case of thermoelastic coupling, the amplitude of the force for the generation of acoustic waves depends on material properties such as elastic constants coefficient of

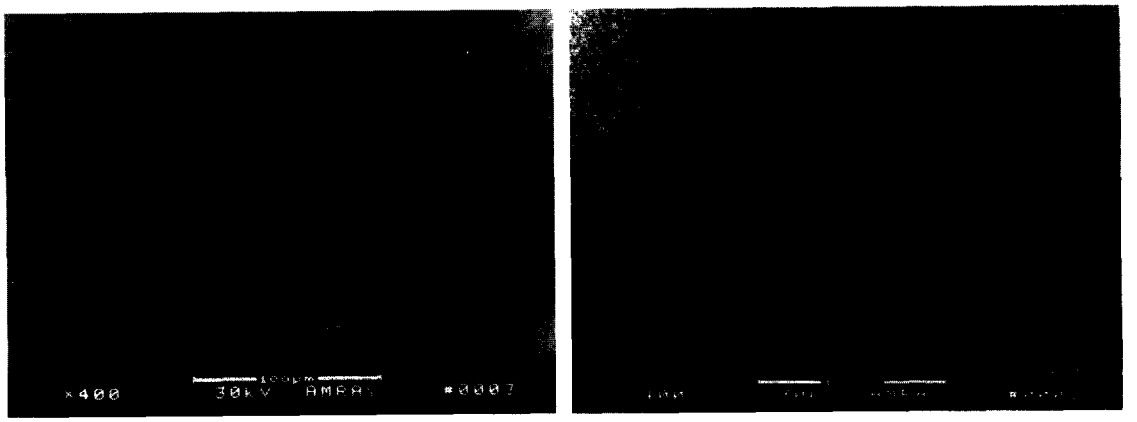

(a) SEM image (b) SEAM image f = 186.2 kHz

Fig. 2. The *n*-GaSb substrate images.

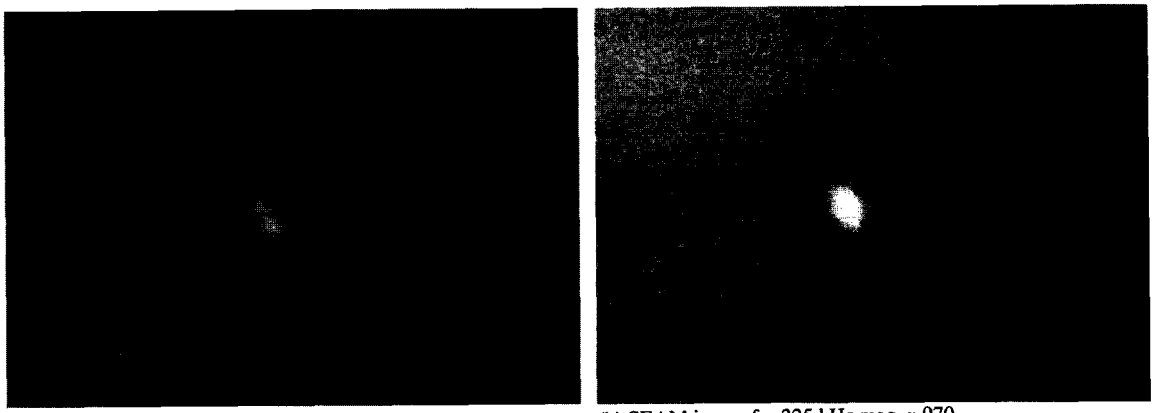

(a) SEM image (b) SEAM image f = 225 kHz mag. x 970

Fig. 3. The GaInAsSb epilayer images on a GaSb substrate.

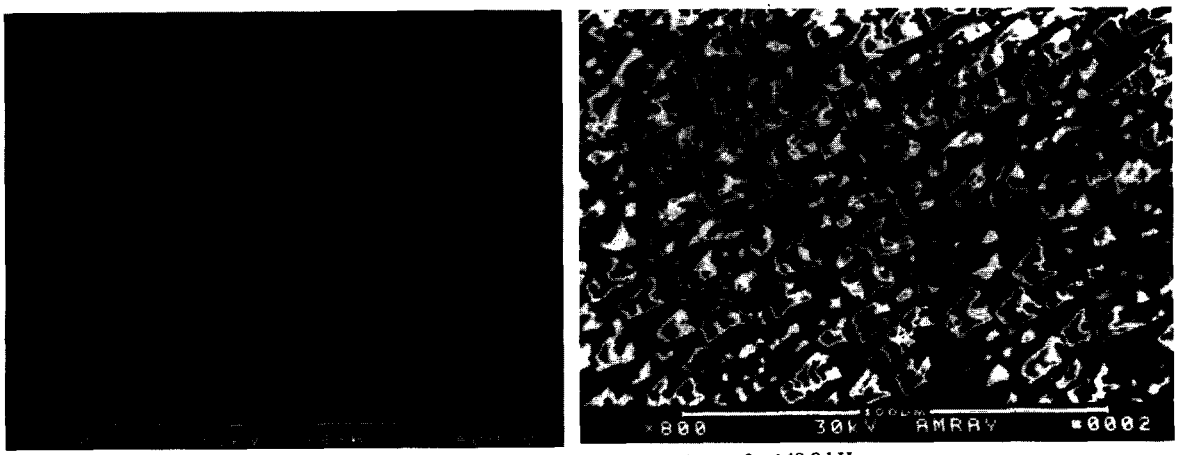

(a) SEM image (b) SEAM image f = 149.8 kHz

Fig. 4. The GaSb epilayer images on a GaAs substrate.

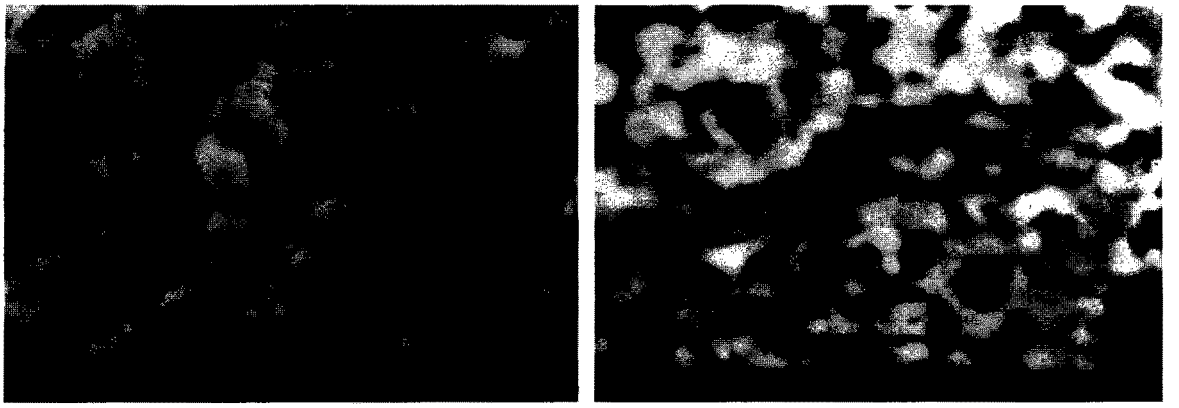

(a) SEM image (b) SEAM image f = 143.5 kHz

Fig. 5. The InSb epilayer images on a GaPs substrate.

thermal expansion, heat capacity and thermal conductivity. Since all these properties depend on temperature the electron acoustic signal will depend on temperature in a different way for different materials [3]. However, evidence has been found of other nonthermal mechanisms such as piezoelectric coupling and excess carrier coupling in semiconductors. In addition to the temperature dependence of electron-acoustic signals, these make the interpretation of SEAM signals in particular difficult and complex. Because GaSb crystal is a face centred cubic Bravais lattice, there is not the piezoelectric coupling at ⟨1 0 0⟩ crystal orientation of the substrate [9].

If one assumes that the themoelastic coupling is the main signal generation mechanism in GaSb crystal under the present observation conditions, a rough estimate of the crystal slab thickness where the signal is generated can be made by calculating the value of the thermal decay length d at different frequency of SEAM. The thermal waves are diffusive waves and are described by the equation for linear heat flow in a semi-infinite solid [10]. By introducing K into the equation $d = (2K/f\rho C)^{0.5}$ (ρ is the density and f is the frequency) the value of d is obtained.

4. OTHER APPLICATIONS OF SEAM

Several different kinds of specimens were chosen to evaluate the detecting ability of SEAM, Figure 3 shows the SEM and SEAM image of the same area of GaInAsSb epilayer on GaSb by metalorganic chemical vapor deposition (MOCVD). The photograph displays distinct contrast in Fig. 3(A) between surface and interface. The crystal surface rises and falls a little, the crystal subsurface in Fig. 3(B) is smooth, and the bright spot in (B) is a defect which changes from the subsurface to the surface. The images in Fig. 4(A, B) are the morphologies of the surface and the subsurface of GaSb epilayer by MOCVD on a GaAs substrate. The image in Fig. 4(A) presents a number of stacking fault pyramids, and the image in Fig. 4(B) illustrates the background and development of these pyramids. The images in Figs. 5(A, B) are the morphologies of the surface and subsurface of a poor InSb epilayer by MOCVD on GaAs substrate, the strong contrast is observed in Fig. 5.

5. CONCLUSIONS

n-GaSb crystals have been studied by scanning electron acoustic microscopy, and contrast mechanisms in imaging are discussed and compared. Electron-acoustic imaging by SEAM has definite advantages as compared with secondary electron imaging which was observed *in situ* with electron-acoustic imaging. The observation by electron-acoustic imaging is much deeper than that of secondary electron imaging, which is especially useful for nondestructive analysis of devices for optics and electronics. In addition, we can also see that SEAM with multi-operation models has some potential applications combining properties studies and structure analysis on some conductor materials.

Acknowledgement – This work was supported by National Advanced Materials Committee of China under grant 863-715-01-02-02.

REFERENCES

1. Brandis, E. and Rosenewaig, A. *Appl. Phys. Lett.* **37,** 1980, 98.
2. Fernandez, P., Llopis, J. and Piqueras, J., *Mater. Chem. Phys.* **24,** 1989, 215.

3. Urchulutegui, M., Piqueras, J. and Llopis, J., *J. Appl. Phys.* **65,** 1989, 2677.
4. Urchulutegui, M. and Piqueras, J., *J. Appl. Phys.* **69,** 1991, 3589.
5. Dominguez-Adame, F. and Piqueras, J., *J. Appl. Phys.* **66,** 1989, 275.
6. Urchulutegui, M., Piqueras, J. and Aroca, C., *Appl. Phys. Lett.* **59,** 1991, 994.
7. Cantrell, J.H. and Qian Menglu, *Appl. Phys. Lett.* **57,** 1990, 1870.
8. Davies, D.G. *Scanning Electron Microsc.* **III,** 1983, 1163.
9. Smith, D.L., *Solid State Commun.* **57,** 1986, 919.
10. Nguyen Tinh and Rosencwaig, A., *Appl. Surf. Sci.* **24,** 1985, 57.